J. Fluid Mech. (1981), *vol.* 102, *pp.* 127–140
Printed in Great Britain

Spatial stability of the non-parallel Bickley jet

By VIJAY K. GARG
Department of Mechanical Engineering, Indian Institute of Technology Kanpur

(Received 26 November 1979)

The spatial stability of the plane, two-dimensional jet flow to infinitesimal disturbances is investigated by taking into account the effects of transverse velocity component and the streamwise variations of the basic flow and of the disturbance amplitude, wave-number and spatial growth rate. This renders the growth rate dependent on the flow variable as well as on the transverse and streamwise co-ordinates. Growth rates for the energy density of the disturbance and the associated neutral curves are provided as a function of the streamwise co-ordinate. Variation of growth rate of the disturbance stream function and streamwise component of velocity with the transverse co-ordinate is also given for different disturbance frequencies and streamwise locations. Results are compared with those for the parallel-flow stability analysis, and also with those for an analysis that accounts for only some of the non-parallel effects. It is found that the critical Reynolds number based on the growth of energy density of the disturbance depends on the streamwise co-ordinate and lies within the range (around 20) found experimentally, while the parallel-flow theory yields a rather low value of 4·0.

1. Introduction

The stability characteristics of the Bickley jet have been studied extensively. However, most of the studies (Curle 1957; Tatsumi & Kakutani 1958; Clenshaw & Elliot 1960; amongst others) treat the jet as a quasi-parallel flow and apply the parallel-flow stability theory only. This results in a critical Reynolds number for the jet flow of 4·0. Obviously at such low Reynolds numbers, the parallel-flow assumption cannot be expected to hold since the transverse velocity component as well as the jet spread and streamwise variations of the mean flow are not negligible. It is therefore essential to consider the jet as non-parallel flow for the stability analysis.

The difficulty in solving for the stability characteristics of a non-parallel flow lies in the evaluation of the eigenvalues of a set of *partial* differential equations. To overcome this difficulty it is generally assumed that the non-parallel effects are of higher order. This has led to several attempts in the last decade or so to find the stability characteristics of such non-parallel flows as the Blasius boundary layer (Barry & Ross 1970; Bouthier 1972, 1973; Ling & Reynolds 1973; Gaster 1974; Saric & Nayfeh 1975; Smith 1979), the divergent channel flow (Eagles & Weissman 1975), the developing axisymmetric jet (Crighton & Gaster 1976), the slowly varying flow between concentric cylinders (Eagles 1977) and the two-dimensional jet and flat-plate wake (Ling & Reynolds 1973). For the Bickley jet, Haaland (1972) and Bajaj & Garg (1977) accounted for only some of the non-parallel effects. In their model, the governing equations are separable and reduce to a modified Orr–Sommerfeld equation. All the non-parallel effects were taken into account by Ling & Reynolds (1973) for the Bickley jet. However, they considered the temporal rather than the more realistic spatial stability problem, and expanded the stream functions of the basic flow and of the disturbance along with the eigenvalues in a power series about a given streamwise location. Their analysis is therefore valid only for a small neighbourhood of that streamwise location. It also neglects downstream variation of the vertical structure of the Orr–Sommerfeld solutions (Gaster 1974).

Herein, we follow Bouthier (1972) and present a non-parallel stability theory for the Bickley jet. This approach provides for perturbations in the wavenumber and spatial growth rate for fixed frequency and Reynolds number; it also yields the local distortion and streamwise variations of the eigenfunction, the wavenumber and the spatial growth rate.

A complication for non-parallel flow is that the various disturbance flow quantities such as the stream function, velocity components, pressure, etc. have different growth rates, and these growth rates are functions of the transverse co-ordinate. This rather surprising situation, in comparison with parallel-flow theory, was demonstrated by Bouthier (1973) using essentially the same method as we use here. For a measure of instability of the Bickley jet, we follow Shen (1961) in using the growth rate of the disturbance mean kinetic-energy density, averaged over time and integrated across the jet.

2. Analysis

For the stability analysis of a two-dimensional, steady, incompressible jet described by the stream function ψ, we take the X co-ordinate along the jet axis and Y normal to it, and introduce dimensionless variables with respect to a reference length L, a reference velocity U_0, and fluid density ρ, so that $x = (X - X_0)/L$, (X_0 being an arbitrary distance downstream of the origin on the jet axis), $y = Y/L$, etc. Taking the stream function of the disturbance as $\psi'(x,y,t)$, the Navier–Stokes equation, after subtracting the mean flow quantities and neglecting the non-linear terms in ψ', yields

$$\frac{\partial}{\partial t}(\nabla^2\psi') + \frac{\partial\psi}{\partial y}\frac{\partial}{\partial x}(\nabla^2\psi') + \frac{\partial}{\partial x}(\nabla^2\psi)\frac{\partial\psi'}{\partial y} - \frac{\partial\psi}{\partial x}\frac{\partial}{\partial y}(\nabla^2\psi') - \frac{\partial}{\partial y}(\nabla^2\psi)\frac{\partial\psi'}{\partial x} = \frac{1}{R}\nabla^4\psi', \tag{2.1}$$

where $R(= U_0L/\nu)$ is the Reynolds number; ν being the constant kinematic viscosity of the fluid. While (2.1) is valid for an infinitesimal disturbance applied to any two-dimensional basic flow, the boundary conditions depend on the particular flow. For the jet flow under consideration, these are

$$\left.\begin{aligned}\psi' &\to 0\\ D\psi' &\to 0\end{aligned}\right\} \quad \text{as} \quad y \to \pm\infty, \tag{2.2}$$

where $D \equiv \partial/\partial y$.

Considering the jet flow as nearly parallel, we introduce an independent variable x_1 in the axial direction, such that

$$x_1 = \epsilon x, \tag{2.3}$$

where ϵ is a small dimensionless parameter characterizing the non-parallel nature of the basic flow; $\epsilon = 0$ for truly parallel flows. The parameter ϵ depends on the flow under study and may be related to R. Also, x_1 and x are the so-called slow and fast scales, respectively. In the expansions that follow, we treat ϵ and R as independent parameters though they are related. By treating them as independent we are in effect solving the problem in the ϵ, R plane, whereas in reality we need only to solve the problem on a line. The real solution is, therefore, contained in the family of fictitious extensions over all ϵ, R.

The velocity components of the basic flow can be written in terms of the stream function $\psi(x_1, y)$ as

$$\frac{\partial \psi}{\partial y} = U(x_1, y)$$

and

$$-\frac{\partial \psi}{\partial x} = -\epsilon \frac{\partial \psi}{\partial x_1} = \epsilon V(x_1, y). \tag{2.4}$$

Since the coefficients of the derivatives of ψ' in (2.1) are functions of x_1 and y only, the disturbance stream function may be taken as

$$\left.\begin{aligned} \psi' &= [\phi_0(x_1, y) + \epsilon\phi_1(x_1, y) + \ldots]\, e^{i\theta}, \\ \text{where}\quad \frac{\partial \theta}{\partial x} &= k_0(x_1), \quad \frac{\partial \theta}{\partial t} = -\omega. \end{aligned}\right\} \tag{2.5}$$

Here ω is the real dimensionless frequency of the disturbance. The real part of k_0 is the dimensionless wavenumber, and the imaginary part of k_0 is the spatial growth rate of the disturbance. Thus, the slow scale is used to describe the relatively slow variation of the basic flow, the wavenumber, spatial growth rate, and disturbance amplitude, while the fast scale is used to describe the relatively rapid, streamwise variation of the travelling-wave disturbance.

In terms of x_1 and θ, the temporal and spatial derivatives transform according to

$$\frac{\partial}{\partial t} = -\omega \frac{\partial}{\partial \theta}, \quad \frac{\partial}{\partial x} = k_0 \frac{\partial}{\partial \theta} + \epsilon \frac{\partial}{\partial x_1}. \tag{2.6}$$

Substituting (2.5) and (2.6) into (2.1) and (2.2), using (2.4), and equating coefficients of like powers of ϵ, we obtain the following.

Order ϵ°:

$$\left.\begin{aligned} L(\phi_0) \equiv [(D^2 - k_0^2)^2 - iR\{(k_0 U - \omega)(D^2 - k_0^2) - k_0 D^2 U\}]\, \phi_0 = 0, \\ \phi_0 \to 0, \quad D\phi_0 \to 0 \quad \text{as} \quad y \to \pm\infty. \end{aligned}\right\} \tag{2.7}$$

Order ϵ:

$$L(\phi_1) = S, \tag{2.8a}$$

$$\phi_1 \to 0, \quad D\phi_1 \to 0 \quad \text{as} \quad y \to \pm\infty, \tag{2.8b}$$

where

$$S = R\left[b_1 \frac{\partial \phi_0}{\partial x_1} + b_2 D^2\left(\frac{\partial \phi_0}{\partial x_1}\right) + b_3 D\phi_0 + VD^3\phi_0 + (b_4\phi_0 - 2iD^2\phi_0/R)\frac{dk_0}{dx_1}\right], \tag{2.8c}$$

$$\left.\begin{aligned} b_1 &= 2k_0\omega - 3Uk_0^2 - D^2 U + 4ik_0^3/R, \\ b_2 &= U - 4ik_0/R, \\ b_3 &= -D^2 V - k_0^2 V, \\ b_4 &= \omega - 3k_0 U + 6ik_0^2/R. \end{aligned}\right\} \tag{2.8d}$$

The eigenvalue problem in (2.7) is the familiar Orr–Sommerfeld problem for parallel flows while (2.8) provides the additional problem arising from the non-parallel effects. The first two terms on the right-hand side of (2.8c) represent the effects of the streamwise variation of the disturbance amplitude, the third and fourth terms represent the effects of the transverse mean velocity component, and the last term represents the effects of the streamwise variation of the wavenumber and spatial growth rate.

3. Solution

The slow scale x_1 appears implicitly in (2.7). For a given ω, R and $U(x_1, y)$, the eigenvalue problem (2.7) can be solved numerically to determine the eigenvalue $k_0(x_1)$, and the solution $\phi_0(x_1, y)$ may be expressed as

$$\phi_0 = C(x_1)\,\xi(y; x_1), \tag{3.1}$$

where ξ is the eigenfunction, and the amplitude function C is unknown at this level of approximation. It will be determined to within a multiple at the next level of approximation. For a truly parallel flow, C would be a constant and (3.1) would be the complete solution.

For the solution of the inhomogeneous problem in (2.8), we invoke the solvability condition that the inhomogeneous terms be orthogonal to every solution of the adjoint homogeneous problem, that is

$$\int_{-\infty}^{\infty} S\xi^*\,dy = 0, \tag{3.2}$$

where $\xi^*(y; x_1)$ is the eigenfunction corresponding to the eigenvalue k_0 of the adjoint problem

$$L^*(\xi^*) \equiv (D^2-k_0^2)^2\,\xi^* - iR[(k_0 U-\omega)\,(D^2-k_0^2)\,\xi^* + 2k_0 DUD\xi^*] = 0, \tag{3.3a}$$

$$\xi^* \to 0, \quad D\xi^* \to 0 \quad \text{as} \quad y \to \pm\infty. \tag{3.3b}$$

Substituting for S from (2.8c) into (3.2) and using (3.1), we get the following equation for $C(x_1)$,

$$\frac{dC}{dx_1} = ik_1(x_1)\,C, \tag{3.4a}$$

where

$$ik_1 = a_2(x_1)/a_1(x_1), \tag{3.4b}$$

$$a_1(x_1) = -\int_{-\infty}^{\infty} (b_1\xi + b_2 D^2\xi)\,\xi^*\,dy, \tag{3.4c}$$

$$a_2(x_1) = \int_{-\infty}^{\infty} [(b_1 + D^2U)\,\xi^* + 2DUD\xi^* + b_2 D^2\xi^*]\frac{\partial\xi}{\partial x_1}\,dy + \int_{-\infty}^{\infty}\left[(b_4\xi - 2iD^2\xi/R)\frac{dk_0}{dx_1} + b_3 D\xi + VD^3\xi\right]\xi^*\,dy, \tag{3.4d}$$

the first term in (3.4d) having been obtained by integration by parts. The solution of (3.4a) is

$$C(x_1) = C_0 \exp\,[i{\textstyle\int} k_1(x_1)\,dx_1] = C_0 \exp\,[i\epsilon{\textstyle\int} k_1(x_1)\,dx], \tag{3.5}$$

where C_0 is a constant of integration. Thus, to first approximation,

$$\psi' = C_0 \xi(y; x_1) \exp\left[i \int (k_0 + \epsilon k_1)\, dx - i\omega t\right], \tag{3.6}$$

where ξ and k_0 are calculated at each axial location as if the basic flow were parallel, and k_1 contains the effects of the transverse velocity component and streamwise variation of the mean flow, the eigenfunction ξ, and the eigenvalue k_0.

In order to determine $a_2(x_1)$, we need to evaluate $\partial\xi/\partial x_1$ and dk_0/dx_1. To do so, we differentiate $L(\xi) = 0$ with respect to x_1, and obtain

$$L\left(\frac{\partial \xi}{\partial x_1}\right) = e_1 + e_2 \frac{dk_0}{dx_1}, \tag{3.7a}$$

with boundary conditions

$$\frac{\partial \xi}{\partial x_1} \to 0, \quad D\left(\frac{\partial \xi}{\partial x_1}\right) \to 0 \quad \text{as} \quad y \to \pm\infty, \tag{3.7b}$$

where

$$\left.\begin{aligned} e_1 &= iRk_0[(k_0^2 DV + D^3 V)\xi - DVD^2\xi], \\ e_2 &= 4k_0(D^2\xi - k_0^2\xi) + iR[UD^2\xi + (2k_0\omega - 3k_0^2 U - D^2 U)\xi]. \end{aligned}\right\} \tag{3.7c}$$

The inhomogeneous problem in (3.7) is solved by invoking the solvability condition that yields

$$\frac{dk_0}{dx_1} = -\int_{-\infty}^{\infty} e_1 \xi^* dy \Big/ \int_{-\infty}^{\infty} e_2 \xi^* dy. \tag{3.8}$$

Knowing dk_0/dx_1 from (3.8), it is a simple matter to evaluate $\partial\xi/\partial x_1$ from the integration of (3.7a).

For a truly parallel basic flow, ξ is a function of y only, $k_1 = 0$, and k_0 is a constant. Hence, the growth rate of any disturbance quantity, such as the velocity, the pressure, and the kinetic energy, is given uniquely by the imaginary part of k_0. On the other hand, the effects of non-parallelism are to make k_0 a function of x_1, to produce a correction $\epsilon k_1(x_1)$ to k_0, and to make the mode shape vary in the streamwise direction. Hence, the streamwise variation of each flow quantity depends on its distance from the jet axis. Moreover, at each distance y, the different flow quantities vary differently in the streamwise direction, as we shall see in § 5.

4. Computational procedure

For the Bickley jet, the axial and transverse components of velocity, according to (2.4), are given by

$$\left.\begin{aligned} U &= f^{\frac{1}{2}} \operatorname{sech}^2 fy, \\ V &= 2f(2fy \operatorname{sech}^2 fy - \tanh fy), \\ f &= (1 + 6x/R^{\frac{1}{2}})^{-\frac{1}{3}}. \end{aligned}\right\} \tag{4.1}$$

where

Since this velocity distribution results from the boundary-layer type of equations for the jet flow, it is obvious that ϵ may be taken as $R^{-\frac{1}{2}}$. The problem describing the eigenfunction ξ is

$$L(\xi) = 0, \tag{4.2a}$$

$$\xi \to 0, \quad D\xi \to 0 \quad \text{as} \quad y \to \pm\infty. \tag{4.2b}$$

Since the jet flow is known to be more unstable to symmetric disturbances (Monin & Yaglom 1971), we may consider the additional conditions at the jet axis for such disturbances, as

$$D\xi = D^3\xi = 0 \quad \text{at} \quad y = 0, \tag{4.3}$$

thereby, reducing the range of integration to $0 \leqslant y \leqslant \infty$ only. The fact that as $y \to \pm\infty$, the variable coefficients in (4.2a) become constant can be utilized in obtaining analytical solution of the asymptotic form of (4.2a). Starting with this analytical solution, (4.2a) is integrated numerically toward the jet axis where satisfaction of the boundary conditions in (4.3) yields the eigenvalue k_0.

The asymptotic form of (4.2a) is

$$[D^4 + (i\omega R - 2k_0^2)\, D^2 + k_0^2(k_0^2 - i\omega R)]\, \xi = 0, \tag{4.4}$$

for as $y \to \pm\infty$, $U \to 0$, $D^2U \to 0$. The linearly independent solutions of (4.4) that satisfy (4.2b) at $y = \infty$ are

$$\xi_1 = \exp(-k_0 y), \quad \xi_2 = \exp(-\alpha_0 y), \quad \alpha_0 = (k_0^2 - i\omega R)^{\frac{1}{2}}. \tag{4.5}$$

Given ω and R, and starting with a guess for k_0 (taken from Bajaj & Garg 1977, figures 4 and 6), and the asymptotic solutions in (4.5) at $y = y_m$, where y_m is some large value of y where conditions applicable to $y = \infty$ may be assumed, Gill's variation of the Runge–Kutta method is used to integrate (4.2a) to $y = 0$, where owing to (4.3), the following condition must hold

$$\begin{vmatrix} D\xi_1(0) & D\xi_2(0) \\ D^3\xi_1(0) & D^3\xi_2(0) \end{vmatrix} = 0. \tag{4.6}$$

The initially assumed value of k_0 is iterated until (4.6) is satisfied. The eigenfunction ξ is then given by

$$\xi = \xi_1 - h(x_1)\, \xi_2, \quad h(x_1) = \frac{D\xi_1(0)}{D\xi_2(0)}. \tag{4.7}$$

With k_0 known, a procedure similar to the one above is used to solve (3.3) for ξ^*; the difference being that no iteraction is required since the adjoint problem has the same eigenvalues as the original problem. This, in fact, serves as a good check on the accuracy of the calculated eigenvalues. It may be noted that the asymptotic form of (3.3a) is the same as (4.4) for ξ, so that (4.5) also gives the linearly independent solutions for ξ^* at $y \geqslant y_m$. For some initial test cases, it was found that at least six significant figures in the eigenvalues of the original and adjoint problems were the same. Later only eigenvalue of the original problem was used to compute adjoint eigenfunctions.

With k_0, ξ, and ξ^* known, dk_0/dx_1 is calculated from (3.8) and (3.7c). The values of $\partial\xi/\partial x_1$ are then given by the integration of (3.7a) from $y = y_m$ to $y = 0$; the necessary starting value at $y = y_m$ being given by the differentiation of ξ in (4.7) as

$$\left.\frac{\partial\xi}{\partial x_1}\right|_{y=y_m} = -\frac{dk_0}{dx_1} y_m\, e^{-k_0 y_m} + \left(h\frac{d\alpha_0}{dx_1} y_m - \frac{dh}{dx_1}\right) e^{-\alpha_0 y_m}. \tag{4.8}$$

As a check on this procedure, (4.2) was solved at three axial locations for constant ω and R, yielding $k_0(x_1)$ and $\xi(y; x_1)$ in each case. Using forward differences, $\delta k_0/\delta x_1$ and $\delta\xi/\delta x_1$ were calculated. It was found that the values of $\delta k_0/\delta x_1$ and dk_0/dx_1 were in agreement to within computational accuracy; also, $\delta\xi/\delta x_1$ and $\partial\xi/\partial x_1$ were in agreement at every point in the flow domain; at least six significant figures being the same.

Calculations were performed in double precision mode on a DEC 1090 computer. The distance y_m from the jet axis, where the asymptotic form of the solution is assumed to hold, was taken to be 6·0 at $x_1 = 0$ and increased appropriately for larger x_1 while the step size for Gill's variation of the Runge–Kutta method was taken as 0.04. For numerical integration, the third-order composite Newton–Cotes quadrature formula (Hildebrand 1974, p. 93) was used. For the determination of dh/dx_1, Δx_1 was taken to be 0·001 and it was noticed that both central and forward differences resulted in at least six correct significant figures for $\delta h/\delta x_1$. It was also found that reducing the step size in either x or y direction by a factor of two resulted in at least six same significant figures. No filtering technique was necessary to keep the two solutions (say ξ_1 and ξ_2) linearly independent owing to the low Reynolds numbers involved.

5. The growth rates

To the first approximation, i.e. to $O(\epsilon)$, the stream function of the disturbance is given by (3.6), which may be rewritten as

$$\psi' = C_0\xi(y; x_1)\exp[i\textstyle\int\alpha dx - i\omega t], \tag{5.1}$$

where $\alpha \equiv k_0 + \epsilon k_1$.

The amplitude of this stream function that may be observed in an experiment is

$$|\psi'| = |C_0|\,|\xi(y; x_1)|\exp(-\textstyle\int\alpha_i dx), \tag{5.2}$$

where α_i is the imaginary part of α. We define a growth rate based on ψ' in x space as

$$g_{\psi'} \equiv \frac{1}{|\psi'|}\frac{\partial|\psi'|}{\partial x}. \tag{5.3}$$

Using (5.2), (5.3) becomes

$$g_{\psi'} = -\alpha_i + \epsilon\frac{1}{|\xi|}\frac{\partial|\xi|}{\partial x_1}. \tag{5.4}$$

We see that the growth rate of the stream function is dependent on the streamwise and transverse co-ordinates since $|\xi|$ is a function of both x_1 and y. Also, when $k_{0i} = 0$, i.e. at the neutral points determined by the parallel flow theory, there is still growth or decay due to the higher-order effects. Thus, the higher-order corrections are essential in determining the correct neutral points.

Another feature of the $O(\epsilon)$ corrections is that the growth rate is different for different flow quantities. Consider, for example, the x component of disturbance velocity, given by

$$u \equiv \frac{\partial\psi'}{\partial y} = C_0\frac{\partial\xi}{\partial y}\exp[i\textstyle\int\alpha\, dx - i\omega t], \tag{5.5}$$

and therefore the growth rate of u is

$$g_u = -\alpha_i + \epsilon\frac{1}{|\partial\xi/\partial y|}\frac{\partial|\partial\xi/\partial y|}{\partial x_1}. \tag{5.6}$$

This is, in general, different from the growth rate of the stream function, given by (5.4). The question then arises about the 'proper' measure for the growth of the disturbance.

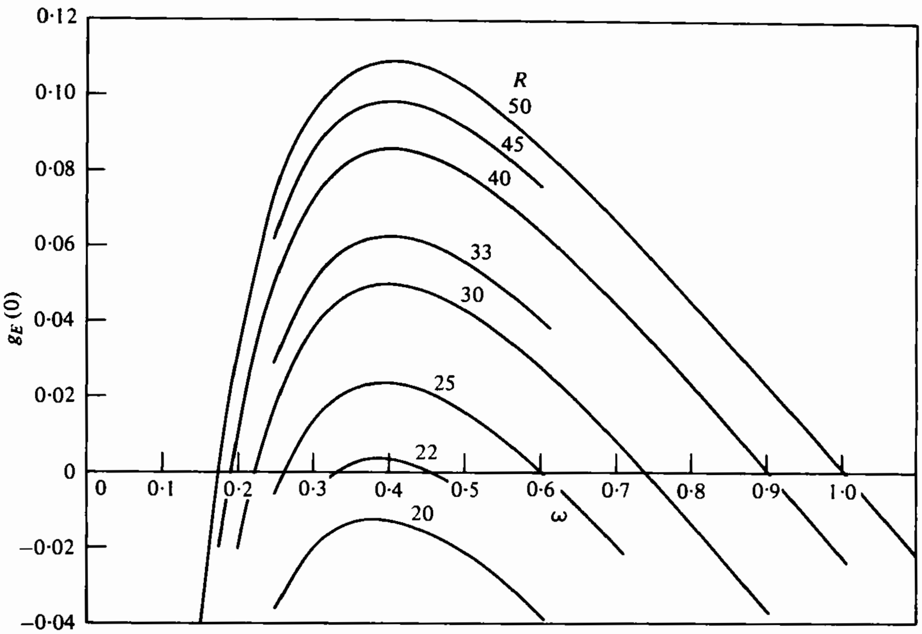

FIGURE 1. Variation of g_E with ω at various R for $x = 0$.

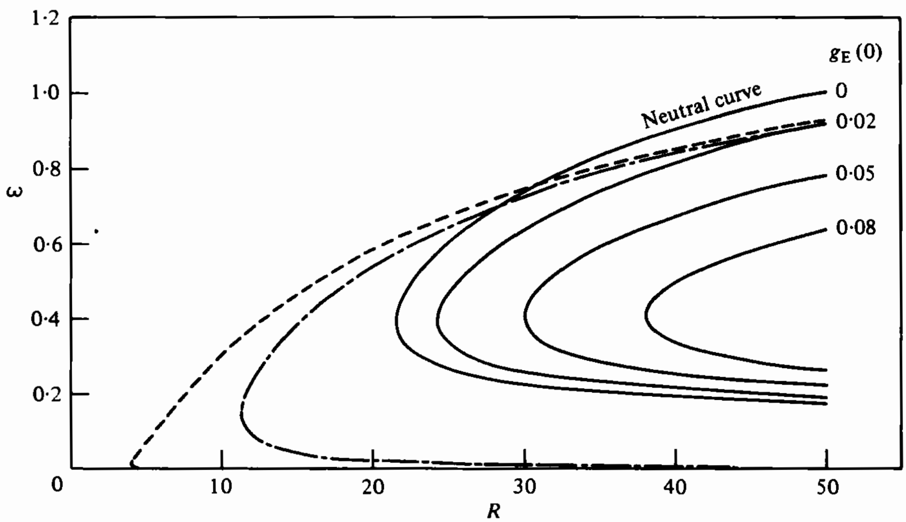

FIGURE 2. Curves of constant growth rates. ——, present results for $g_E(0)$; – – –, neutral curve ($k_{0i} = 0$) based on parallel-flow theory; —–—, neutral curve based on theory A.

If one has experimental data to compare with the calculations, one must obviously use the same quantity as that which was observed. For the stability of the Bickley jet at low Reynolds numbers, Sato & Sakao (1964) do present some experimental results but they themselves point out the difficulty of comparing their results with theoretical predictions. In order to compare the present results with those obtained by the parallel-flow theory, a general measure of the strength of the disturbance as it develops

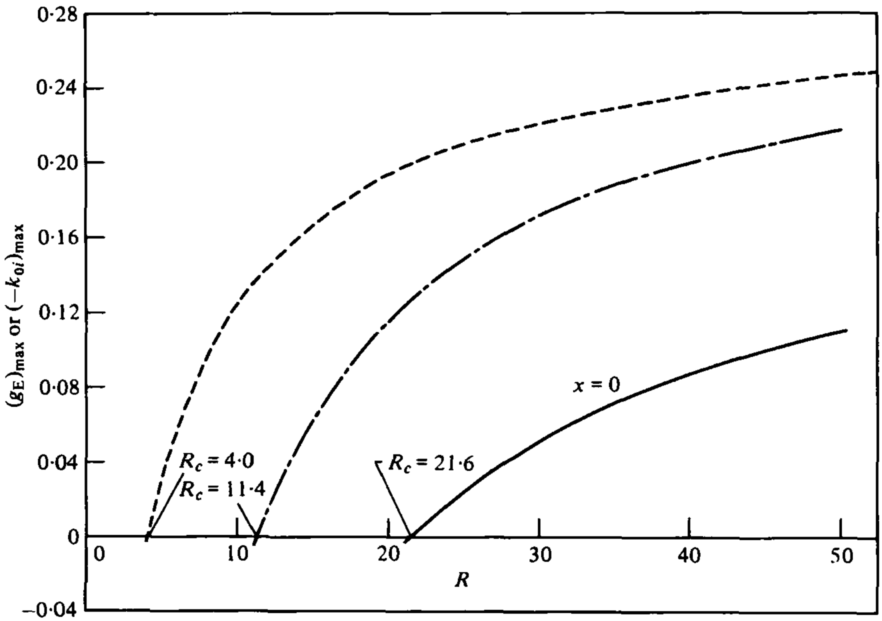

FIGURE 3. Variation of maximum growth rate with R. ——, present results for $g_E(0)_{max}$; – – –, $(-k_{0i})_{max}$ based on parallel-flow theory; — – —, results based on theory A.

downstream is taken to be the mean kinetic energy density, averaged over time and integrated across the jet, defined as:

$$E \equiv \frac{1}{2}\int_{-\infty}^{\infty} (\overline{u^2}+\overline{v^2})\, dy, \tag{5.7}$$

where v is the y component of the disturbance velocity, and an overbar indicates an average over a period.

For growth rate based on E, we should include a factor of a half in the definition to enable comparison with the other growth rates; that is,

$$g_E(x) \equiv \frac{1}{2}\frac{1}{E}\frac{dE}{dx} = -\alpha_i + \frac{\epsilon}{2}\frac{\partial A/\partial x_1}{A}, \tag{5.8}$$

where
$$A = \int_{-\infty}^{\infty} (|D\xi|^2 + |k_0|^2\,|\xi|^2)\, dy.$$

6. Results

For various values of R, ω and streamwise distance x or x_1, growth rates of the disturbance energy density, stream function and streamwise component of velocity were calculated. Most of the results presented here are, however, for g_E only, since the other growth rates depend on the transverse co-ordinate as well. Also, extensive comparison with experimental data (Sato & Sakao 1964) is not possible.

Figure 1 shows the growth rate of energy density at $x = 0$ as a function of the disturbance frequency at various Reynolds numbers and figure 2 shows curves of constant growth rates based on $g_E(0)$. For comparison sake, the latter also has neutral curves,

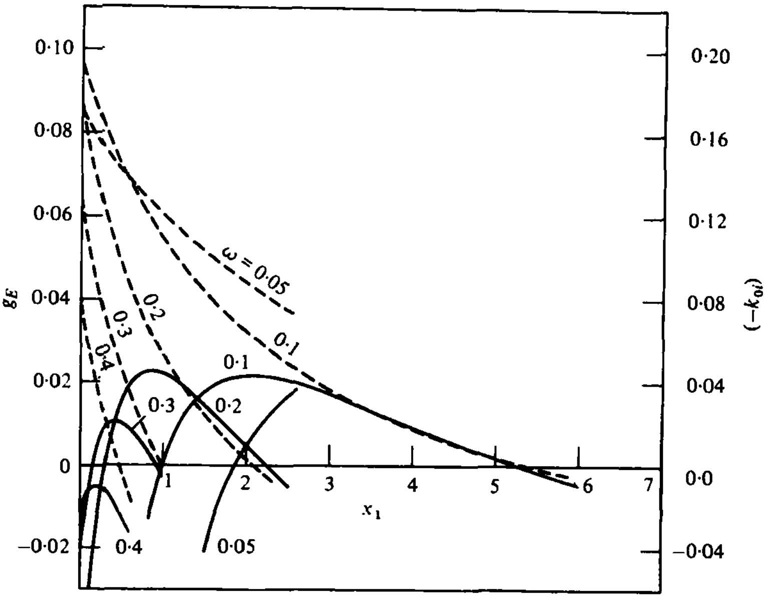

FIGURE 4. Variation of growth rates with streamwise distance for various frequencies at $R = 20$. ——, g_E; – – –, $(-k_{0i})$.

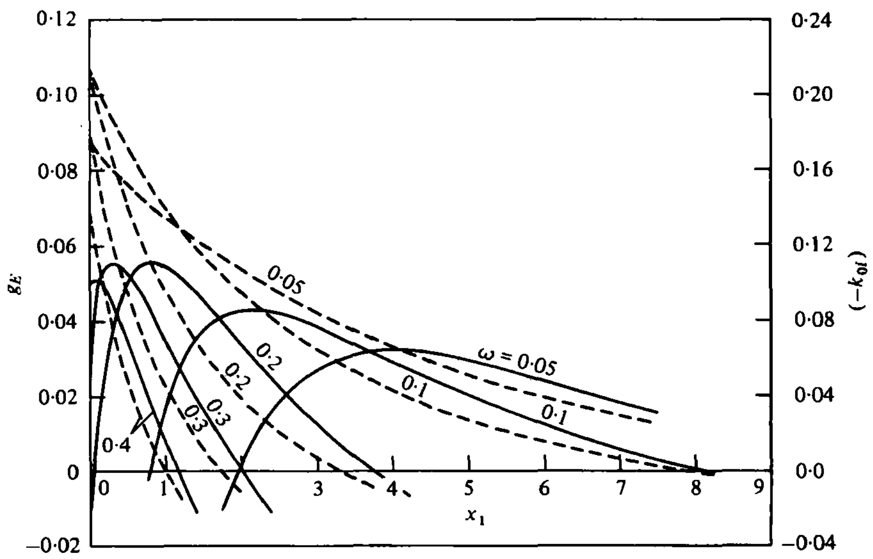

FIGURE 5. Variation of growth rates with streamwise distance for various frequencies at $R = 30$. ——, g_E; – – –, $(-k_{0i})$.

corresponding to $k_{0i} = 0$, for the parallel-flow theory and also for a theory (hereafter called theory A) that accounts for only some of the non-parallel effects (Bajaj & Garg 1977). The differences between the various theories are obvious. In figure 3 are plotted the maxima points on the curves of figure 1 and on similar curves for $(-k_{0i})$ based on the parallel-flow theory and theory A. The present theory yields a critical Reynolds

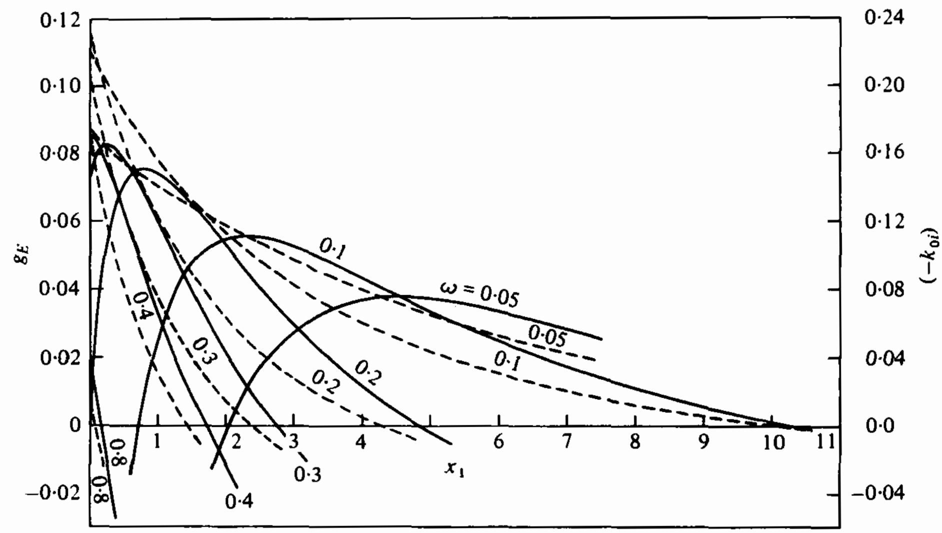

FIGURE 6. Variation of growth rates with streamwise distance for various frequencies at $R = 40$. ——, g_E; – – –, $(-k_{0i})$.

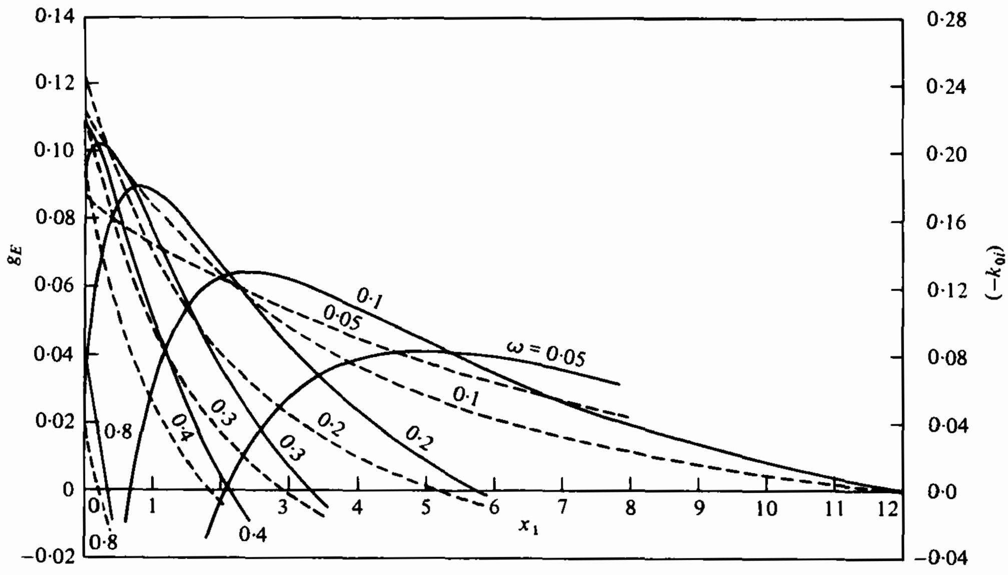

FIGURE 7. Variation of growth rates with streamwise distance for various frequencies at $R = 50$. ——, g_E; – – –, $(-k_{0i})$.

number, $R_c = 21{\cdot}6$ at $x = 0$, which agrees very well with the experimental observation (Sato & Sakao 1964) that the Bickley jet is stable to infinitesimal disturbances below a Reynolds number of 20. In comparison, the parallel-flow theory and theory A yield lower critical Reynolds numbers. Ling & Reynolds (1973) found the Bickley jet to be unstable at all Reynolds numbers. However, they themselves doubt the validity of their theoretical prediction.

Figures 4 to 7 show the variation of g_E and $(-k_{0i})$ with streamwise distance for

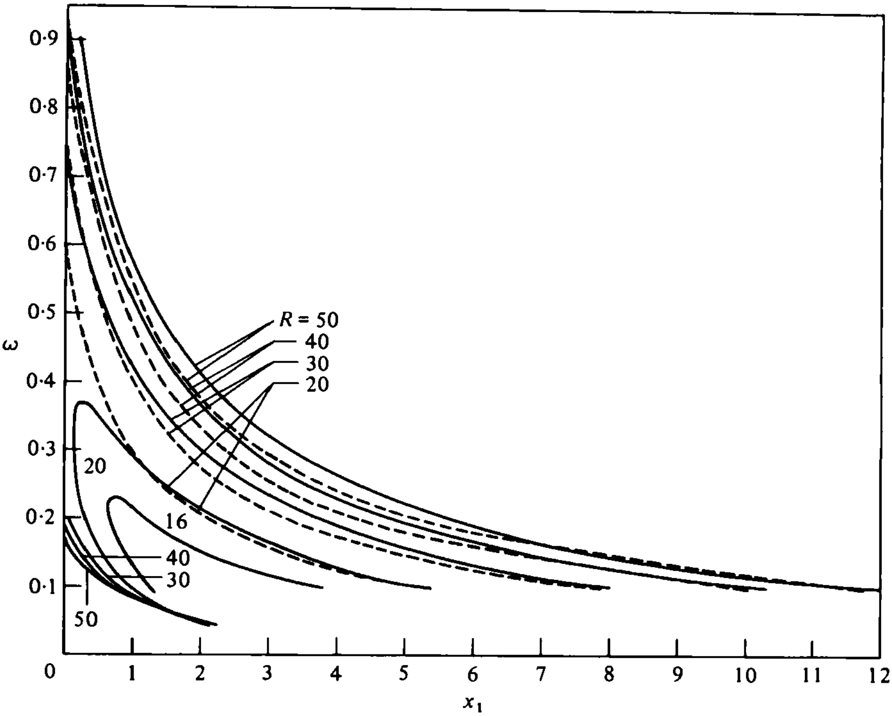

FIGURE 8. Neutral curves (ω *vs.* x_1) at various R. ——, based on g_E; – – –, based on k_{0i}.

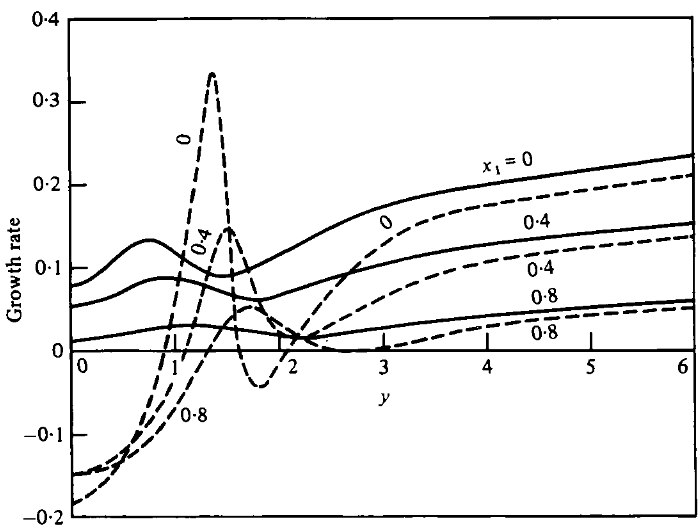

FIGURE 9. Variation of growth rates with transverse co-ordinate for $R = 30$ and $\omega = 0{\cdot}4$ at $x_1 = 0$, 0·4 and 0·8. ——, $g_{\psi'}$; – – –, g_u.

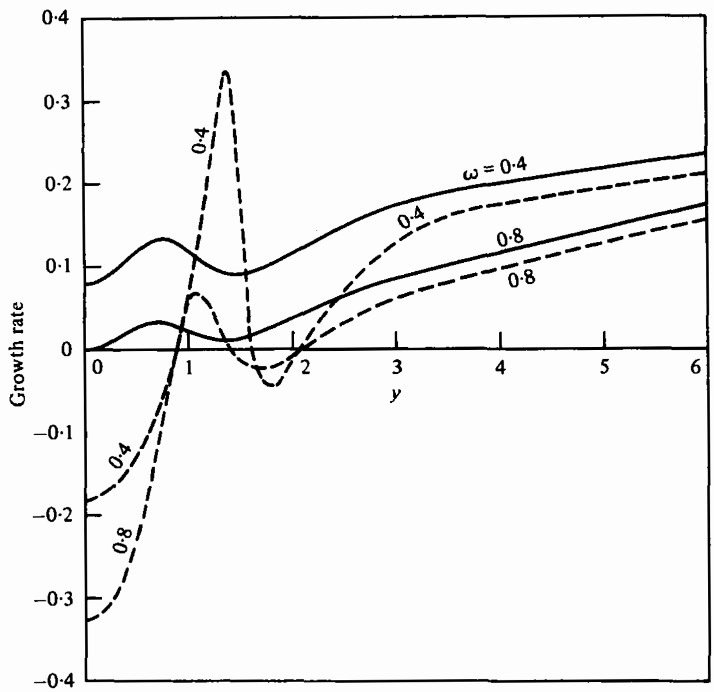

FIGURE 10. Variation of growth rates with transverse co-ordinate for $R = 30$ and $\omega = 0{\cdot}4$ and $0{\cdot}8$ at $x = 0$. ——, $g_{\psi'}$; – – –, g_u.

various ω and $R = 20$, 30, 40 and 50 respectively. It is evident that while $(-k_{0i})$, the growth rate based on the parallel-flow theory, is maximum at $x = 0$ and decreases as x increases, the growth rate of energy density for disturbances of low frequency ($\omega < 0{\cdot}4$) reaches a maximum at $x > 0$. For frequencies greater than 0·4, however, g_E is also maximum at $x = 0$. Note that the abscissa in these figures is $x_1 = \epsilon x$.

Figure 8 shows the neutral curves, corresponding to both $g_E = 0$ and $k_{0i} = 0$, at various R. It is evident that the critical Reynolds number based on g_E depends on the streamwise co-ordinate. Sato & Sakao (1964) do point out the difficulty in finding R_c experimentally. This figure also shows that as x_1 increases, critical Reynolds number and frequency decrease, e.g. for $\omega = 0{\cdot}4$, $R_c = 21{\cdot}6$ at $x_1 = 0$ (figures 2 and 3); for $\omega = 0{\cdot}23$, $R_c = 16$ at $x_1 = 0{\cdot}75$; and for $\omega = 0{\cdot}07$, $R_c \simeq 13$ at $x_1 \simeq 3{\cdot}0$ (not shown). However, it is futile to compute results for lower ω and R as the present analysis is only accurate upto $O(\epsilon)$, where $\epsilon = R^{-\frac{1}{2}}$. From the data provided in figures 4–7, one can also plot neutral curves (ω *vs* R) at various streamwise locations, similar to those in figure 2 at $x = 0$. Figures 9 and 10 show the variation of the growth rate of the disturbance stream function and streamwise component of velocity with the transverse co-ordinate at $R = 30$ for various ω and x_1. Similar behaviour is found at other Reynolds numbers. It can be noted that, in general, as x or ω increases, the growth rates, $g_{\psi'}$ and g_u, decrease for almost all y. Also, the disturbance may pass through regions of growth and regions of decay. Moreover, the stream function of the disturbance may be growing at some point in the jet while the velocity components are decaying.

7. Conclusions

The spatial stability of the non-parallel Bickley jet to infinitesimal disturbances is investigated. The solution takes into account the effects of transverse velocity component and the streamwise variations of the basic flow and of the disturbance amplitude, wavenumber and growth rate. This makes the results quite different from those obtained by the parallel-flow theory. One of the differences is that the (spatial) growth rate becomes a function of the transverse as well as streamwise co-ordinate. Thus, the disturbance may pass through regions of growth and regions of decay. Another striking difference is that the growth rate is a function of the flow quantity involved, i.e. the stream function, velocity components, kinetic energy, etc. For example, the stream function may be growing at some point in the jet while the velocity components are decaying. This leads to different critical Reynolds numbers for different flow quantities.

The present results are found to be in closer agreement with the experimental results than those found earlier by the parallel-flow theory or by a theory that accounted for only a few of the non-parallel effects.

The author is indebted to the reviewers for their valuable comments.

REFERENCES

Bajaj, A. K. & Garg, V. K. 1977 *J. Appl. Mech.* **44**, 378.
Barry, M. D. J. & Ross, M. A. S. 1970 *J. Fluid Mech.* **43**, 813.
Bouthier, M. 1972 *J. Mec.* **11**, 599.
Bouthier, M. 1973 *J. Mec.* **12**, 75.
Clenshaw, C. W. & Elliot, D. A. 1960 *Quart. J. Mech. Appl. Math.* **13**, 300.
Crighton, D. G. & Gaster, M. 1976 *J. Fluid Mech.* **77**, 397.
Curle, N. 1957 *Proc. Roy. Soc.* A **238**, 489.
Eagles, P. M. 1977 *Proc. Roy. Soc.* A **355**, 209.
Eagles, P. M. & Weissman, M. A. 1975 *J. Fluid Mech.* **69**, 241.
Gaster, M. 1974 *J. Fluid Mech.* **66**, 465.
Haaland, S. E. 1972 Ph.D. thesis, University of Minnesota, Minneapolis.
Hildebrand, F. B. 1974 *Introduction to Numerical Analysis*, 2nd edn. McGraw-Hill.
Ling, C. H. & Reynolds, W. C. 1973 *J. Fluid Mech.* **59**, 571.
Monin, A. S. & Yaglom, A. M. 1971 *Statistical Fluid Mechanics*, vol. I, p. 139. Massachusetts Institute of Technology Press.
Saric, W. S. & Nayfeh, A. H. 1975 *Phys. Fluids* **18**, 945.
Sato, H. & Sakao, F. 1964 *J. Fluid Mech.* **20**, 337.
Shen, S. F. 1961 *J. Aero. Sci.* **28**, 397.
Smith, F. T. 1979 *Proc. Roy. Soc.* A **366**, 91.
Tatsumi, T. & Kakutani, T. 1958 *J. Fluid Mech.* **4**, 261.